Inhibition of midkine alleviates experimental autoimmune encephalomyelitis through the expansion of regulatory T cell population

Jinyan Wang*, Hideyuki Takeuchi*†, Yoshifumi Sonobe*, Shijie Jin*, Tetsuya Mizuno*, Shin Miyakawa‡, Masatoshi Fujiwara‡, Yoshikazu Nakamura§¶, Takuma Kato‖, Hisako Muramatsu**, Takashi Muramatsu**††, and Akio Suzumura*†

*Department of Neuroimmunology, Research Institute of Environmental Medicine, Nagoya University, Furo-cho, Chikusa-ku, Nagoya 464-8601, Japan; ‡RIBOMIC, Inc., 3-15-5-601 Shirokanedai, Minato-ku, Tokyo 108-0071, Japan; §Department of Basic Medical Sciences, Institute of Medical Science, University of Tokyo, Shirokanedai, Minato-ku, Tokyo 108-8639, Japan; ¶Core Research Evolutional Science and Technology, Japan Science and Technology Agency, Toyonaka, Osaka 560-8531, Japan; ‖Department of Bioregulation, Mie University Graduate School of Medicine, Tsu, Mie 514-8507, Japan; **Department of Biochemistry, Nagoya University Graduate School of Medicine, Tsurumai-cho, Showa-ku, Nagoya 466-8550, Japan; and ††Department of Health Science, Faculty of Psychological and Physical Sciences, Aichi Gakuin University, Nisshin, Aichi 470-0195, Japan

Edited by Ethan Shevach, National Institutes of Health, Bethesda, MD, and accepted by the Editorial Board January 20, 2008 (received for review October 12, 2007)

$CD4^+CD25^+$ regulatory T (Treg) cells are crucial mediators of autoimmune tolerance. The factors that regulate Treg cells, however, are largely unknown. Here, we show that deficiency in midkine (MK), a heparin-binding growth factor involved in oncogenesis, inflammation, and tissue repair, attenuated experimental autoimmune encephalomyelitis (EAE) because of an expansion of the Treg cell population in peripheral lymph nodes and decreased numbers of autoreactive T-helper type 1 (T_H1) and T_H17 cells. MK decreased the Treg cell population *ex vivo* in a dose-dependent manner by suppression of STAT5 phosphorylation that is essential for Foxp3 expression. Moreover, administration of anti-MK RNA aptamers significantly expanded the Treg cell population and alleviated EAE symptoms. These observations indicate that MK serves as a critical suppressor of Treg cell expansion, and inhibition of MK using RNA aptamers may provide an effective therapeutic strategy against autoimmune diseases, including multiple sclerosis.

aptamer | multiple sclerosis

Midkine (MK), a heparin-binding growth factor, exerts pleiotropic effects, including cell proliferation, cell migration, angiogenesis, and fibrinolysis, in a variety of tissues (1). MK also plays important roles in the induction of oncogenesis, inflammation, and tissue repair. The overexpression of MK has been observed in a number of malignant tumors (1). However, MK-deficient mice are reportedly resistant to ischemic renal injury (2) and neointima formation in atherosclerosis (3). A recent study proposed that MK deficiency suppresses the development of a rheumatoid arthritis model by preventing inflammatory leukocyte migration and osteoclast differentiation (4). Furthermore, MK expression is up-regulated in the spinal cord during the induction and progression phases of experimental autoimmune encephalomyelitis (EAE) (5). However, the precise immunological functions of MK have yet to be elucidated.

Multiple sclerosis (MS) and its animal model, EAE, are autoimmune diseases characterized by inflammatory demyelination in the CNS (6). Although MS and EAE have been described as T-helper type 1 (T_H1) cell-mediated autoimmune diseases, T_H17 cells, a newly discovered lineage of $CD4^+$ T cells that secrete IL-17, have recently been found to be critical for the development of autoimmune diseases, including EAE (7–10). Various types of immune cells and soluble mediators contribute to the complex mechanism underlying the onset and progression of MS, which is characterized by autoreactive T cell infiltration and the activation of microglia, the resident antigen-presenting cells in the CNS. In particular, $CD4^+CD25^+$ regulatory T (Treg) cells have received a great deal of attention as negative regulators of MS pathogenesis (11–14). Treg cells regulate peripheral tolerance and autoimmunity, and abnormalities in Treg cell function may contribute to the development of autoimmune diseases (15–17). Thus, expansion of the Treg cell population could prevent autoimmune attacks, including EAE (12–14, 18, 19).

Here, we show that MK deficiency attenuates myelin oligodendrocyte glycoprotein (MOG)-induced EAE due to an expansion of the Treg cell population in the peripheral lymph nodes, followed by decreases in the numbers of autoreactive T_H1 and T_H17 cells. Moreover, administration of anti-MK RNA aptamers that effectively neutralize MK induced expansion of the Treg cell population and reduced the symptoms of EAE. This demonstrates that MK is a critical suppressor of Treg cell expansion. Moreover, inhibition of MK using RNA aptamers may be a potent therapeutic strategy against autoimmune diseases, including MS.

Results

MK Deficiency Attenuates MOG-Induced EAE. To examine the immunological roles of MK, we generated $MOG_{35–55}$-induced EAE in C57BL/6J WT and MK-deficient ($Mdk^{-/-}$) mice. Most of the WT mice exhibited clinical signs of the disease ≈12 days after the initial immunization and developed peak EAE ≈18 days after immunization as described previously (20, 21). Almost all of the $Mdk^{-/-}$ mice also developed EAE. However, the clinical scores of the $Mdk^{-/-}$ mice were significantly lower than those of the WT mice (Fig. 1*a*).

To confirm whether the suppression of EAE in the $Mdk^{-/-}$ mice was due to MK deficiency, we administrated MK to the $Mdk^{-/-}$ mice with s.c.-implanted microosmotic pumps for ≈16 days after MOG immunization as described previously (3, 4). As shown in Fig. 1, MK administration to $Mdk^{-/-}$ mice abolished the suppression of EAE ($Mdk^{-/-}$ + MK) (Fig. 1*a*). However, the cessation of MK administration resulted in regaining the attenuation of EAE in $Mdk^{-/-}$ + MK mice (starting 22 days after MOG immunization).

Histological analysis of the lumbar spinal cord revealed that

Author contributions: J.W., H.T., and Y.S. contributed equally to this work; H.T. and A.S. designed research; J.W., H.T., Y.S., S.J., T.M., and T.K. performed research; S.M., M.F., Y.N., H.M., and T.M. contributed new reagents/analytic tools; J.W., H.T., and Y.S. analyzed data; and H.T. and A.S. wrote the paper.

The authors declare no conflict of interest.

This article is a PNAS Direct Submission. E.S. is a guest editor invited by the Editorial Board.

Freely available online through the PNAS open access option.

†To whom correspondence may be addressed. E-mail: htake@riem.nagoya-u.ac.jp or suzumura@riem.nagoya-u.ac.jp.

This article contains supporting information online at www.pnas.org/cgi/content/full/0709592105/DC1.

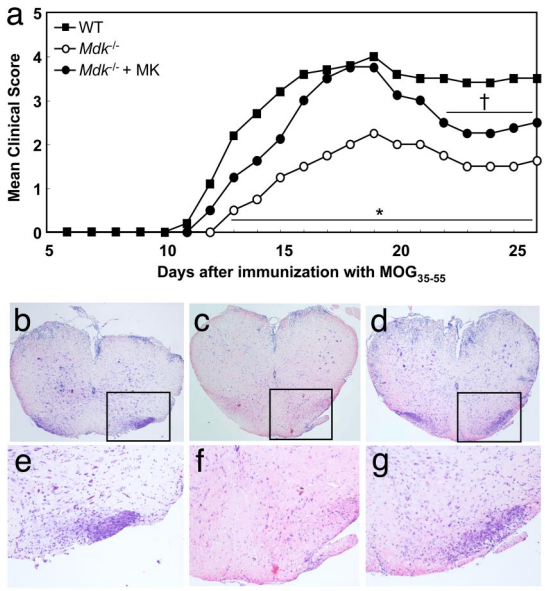

Fig. 1. Attenuation of MOG-induced EAE in MK-deficient mice. (*a*) EAE clinical scores for WT (filled squares; $n = 16$), $Mdk^{-/-}$ (open circles; $n = 13$), and MK-administered $Mdk^{-/-}$ mice ($Mdk^{-/-}$ + MK) (filled circles; $n = 13$). $Mdk^{-/-}$ mice exhibited significantly lower clinical scores than WT mice (*, $P < 0.01$ vs. WT). MK administration to $Mdk^{-/-}$ mice abrogated the attenuation of EAE. After MK administration ceased (starting 22 days after MOG immunization), $Mdk^{-/-}$ + MK mice showed the partial suppression of EAE symptoms again (†, $P < 0.05$ vs. WT). (*b–g*) H&E staining of lumbar spinal cords from peak EAE mice. *e*, *f*, and *g* are higher-magnification images of the boxed areas in *b*, *c*, and *d*, respectively. (Original magnification: *b–d*, ×100; *e–g*, ×400.) (*b* and *e*) WT mice (score, 5) showed inflammatory cell infiltration in the spinal cord. (*c* and *f*) In contrast, only a few infiltrating cells were observed in $Mdk^{-/-}$ mice (score, 2). (*d* and *g*) $Mdk^{-/-}$ + MK mice (score, 5) exhibited inflammatory cell infiltration that was similar to that observed in WT mice.

$Mdk^{-/-}$-EAE mice had fewer infiltrating inflammatory cells than WT-EAE mice (WT mice) (Fig. 1 *b* and *e*) ($Mdk^{-/-}$ mice) (Fig. 1 *c* and *f*). MK administration also reversed this reduced level of CNS inflammation in the $Mdk^{-/-}$ mice ($Mdk^{-/-}$ + MK mice) (Fig. 1 *d* and *g*). These histological findings agreed with the clinical data.

Taken together, these data indicate that MK plays an important role in the induction and development of EAE and that these immunological effects of MK are transient and reversible.

MK Deficiency Induces the Expansion of the $CD4^+CD25^+Foxp3^+$ Treg Cell Population in Peripheral Lymph Nodes. We then assessed the immunological differences between WT and $Mdk^{-/-}$ mice after MOG immunization. First, we compared the expression profiles of antigen-presenting molecules [MHC class II, B7–1, B7–2, intercellular adhesion molecule (ICAM)-1, and vascular cell adhesion molecule (VCAM)-1], cytokines (TNF-α, IL-1β, IL-6, TGF-β, and IL-12), chemokines [IFN-γ-inducible 10-kDa protein (IP-10) regulated upon activation normal T cells expressed and secreted (RANTES), macrophage inflammatory protein-1α (MIP-1α), and monocyte chemoattractant protein-1 (MCP-1)], and iNOS in microglia or macrophages (as the antigen-presenting cells in the CNS or periphery, respectively). Before stimulation with LPS and IFN-γ, $Mdk^{-/-}$ microglia had higher B7–2, MCP-1, and IL-1β expression levels and lower ICAM-1 and MIP-1α expression levels than WT microglia. In contrast, $Mdk^{-/-}$ macrophages had higher B7–1 and B7–2 expression levels than WT macrophages. After stimulation with LPS and IFN-γ, however, these differences were no longer observed, except for decreased expression of VCAM-1 and MIP-1α in $Mdk^{-/-}$ microglia [supporting information (SI) Fig. 6*a*]. The total number of mononuclear cells from the peripheral lymph nodes was similar between WT and $Mdk^{-/-}$ mice (data not shown). Thus, we assessed subpopulations of T cells in the peripheral lymph nodes. No significant differences were found between WT and $Mdk^{-/-}$ mice in the $CD4^+$ and $CD8^+$ T cell populations (SI Fig. 6 *b–d*). Interestingly, however, the $CD4^+CD25^+$ T cell populations had undergone a significant expansion in the $Mdk^{-/-}$-EAE mice, compared with those in the WT-EAE mice (Fig. 2 *a* and *b*). This

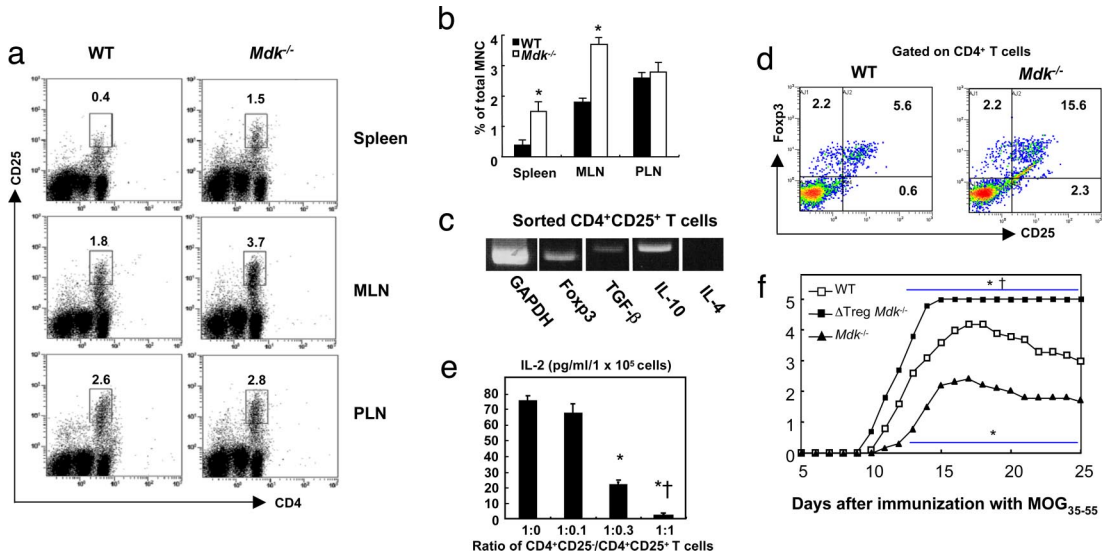

Fig. 2. Expansion of the $CD4^+CD25^+Foxp3^+$ Treg cell population in the peripheral lymph nodes of MOG-immunized mice. (*a*) Flow-cytometric characterization of the $CD4^+CD25^+$ T cells from the spleens, mesenteric lymph nodes (MLN), and popliteal lymph nodes (PLN) at the onset of EAE (12–14 days after immunization) in WT and $Mdk^{-/-}$ mice. (*b*) The percentages of $CD4^+CD25^+$ T cells among all of the mononuclear cells. Data represent the means ± SD ($n = 5$). *, $P < 0.05$ versus WT. (*c*) RT-PCR analysis of *Foxp3* and inhibitory cytokine profiles for purified $CD4^+CD25^+$ T cells from $Mdk^{-/-}$ mice. (*d*) Flow-cytometric analysis of $CD4^+CD25^+Foxp3^+$ T cells in spleens from WT and $Mdk^{-/-}$ mice. (*e*) Suppression of $CD4^+CD25^-$ T cell proliferation by $CD4^+CD25^+$ T cells determined as a function of IL-2 production. Data represent the means ± SD ($n = 5$). *, $P < 0.05$ versus 1:0. †, $P < 0.05$ versus 1:0.3. (*f*) EAE clinical scores of WT, $Mdk^{-/-}$, and Treg cell-depleted $Mdk^{-/-}$ mice. Treg cell depletion in $Mdk^{-/-}$ mice abolished the suppression of EAE (WT mice, open squares; $Mdk^{-/-}$ mice, filled triangles; Treg cell-depleted $Mdk^{-/-}$ mice, filled squares; $n = 5$ for each group). *, $P < 0.05$ versus WT mice. †, $P < 0.01$ versus $Mdk^{-/-}$ mice.

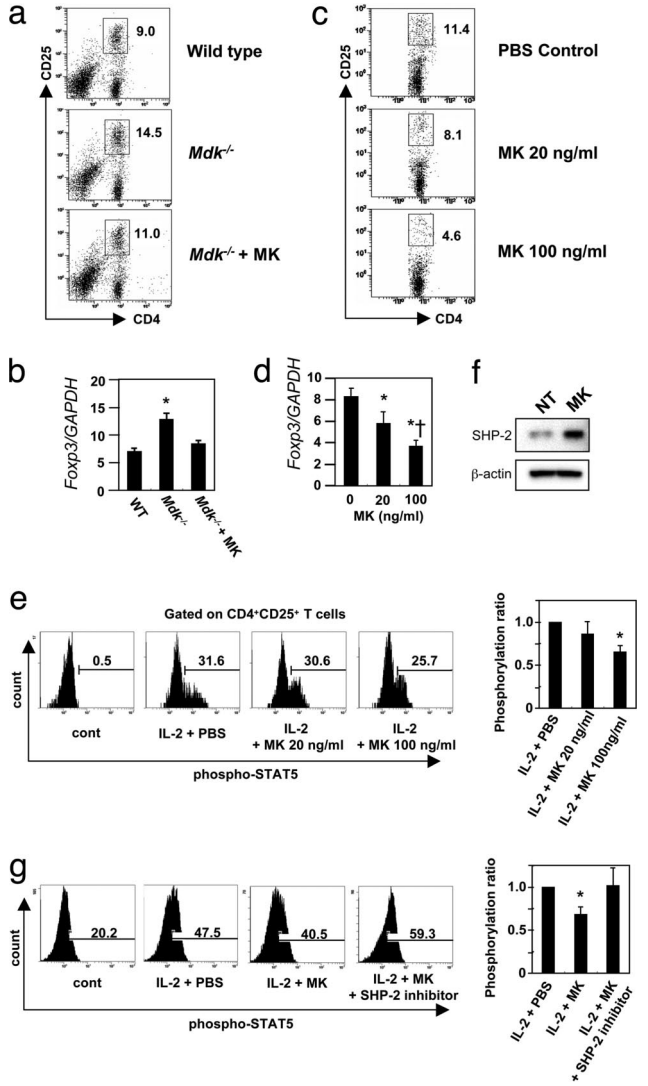

Fig. 3. MK decreases the Treg cell percentage *in vitro* and *in vivo*. (*a*) Flow-cytometric analysis of the Treg cell population in spleens from WT, $Mdk^{-/-}$, or MK-administered $Mdk^{-/-}$ ($Mdk^{-/-}$ + MK) mice at the onset of EAE (12–14 days after immunization). (*b*) Real-time RT-PCR analysis of the *Foxp3* mRNA expression level in purified $CD4^+$ T cells. *Foxp3* expression levels are shown relative to those of *GAPDH*. Data represent the means ± SD ($n = 3$). *, $P < 0.05$ versus WT. (*c*) Suppression of the Treg cell population by MK. Splenic $CD4^+$ T cells from WT EAE mice were stimulated with $MOG_{35–55}$ in the presence of 0–100 ng/ml MK. (*d*) Real-time RT-PCR analysis of the *Foxp3* mRNA expression level in purified $CD4^+$ T cells. *Foxp3* expression levels are shown relative to those of *GAPDH*. Data represent the means ± SD ($n = 3$). *, $P < 0.05$ versus PBS. †, $P < 0.05$ versus 20 ng/ml MK. (*e*) Suppression of STAT5 phosphorylation in $CD4^+CD25^+$ T cells by MK. Splenocytes from WT mice were stimulated with IL-2 for 15 min in the presence of 0–100 ng/ml MK. Representative flow-cytometric data in three independent experiments are demonstrated. STAT5 phosphorylation levels are shown relative to those of IL-2 plus PBS. Data represent the means ± SD ($n = 3$). *, $P < 0.05$ versus IL-2 + PBS. (*f*) Western blotting analysis of SHP-2 expression in purified $CD4^+CD25^+$ T cells treated with or without 100 ng/ml MK. Representative data in three independent experiments are demonstrated. (*g*) Inhibition of SHP-2 restored STAT5 phosphorylation suppressed by MK. Purified $CD4^+CD25^+$ T cells from WT mice were stimulated with IL-2 and 0–100 ng/ml MK with or without SHP-2 inhibitor. Representative flow-cytometric data in three independent experiments are demonstrated. STAT5 phosphorylation levels are shown relative to those of IL-2 plus PBS. Data represent the means ± SD ($n = 3$). *, $P < 0.05$ versus IL-2 plus PBS.

difference of $CD4^+CD25^+$ T cell populations was not detected between WT and $Mdk^{-/-}$ mice without immunization (data not shown). This T cell subpopulation was found to express TGF-β, IL-10, and forkhead box protein P3 (Foxp3) (Fig. 2 *c* and *d*), and it suppressed the antigen-specific expansion of the $CD4^+CD25^-$ T cell population in a titer-dependent manner (Fig. 2*e*). Thus, these cells were identified as $CD4^+CD25^+Foxp3^+$ Treg cells. Depletion of Treg cells from $Mdk^{-/-}$ mice via the administration of anti-CD25 monoclonal antibodies abolished the suppression to EAE in these mice (Fig. 2*f* and SI Fig. 7). Moreover, MK administration in $Mdk^{-/-}$ mice markedly inhibited the increase in the number of Treg cells and the corresponding increase in *Foxp3* expression (Fig. 3 *a* and *b*). These findings demonstrated that MK deficiency transiently recruits an expanded population of Treg cells to the peripheral lymph nodes after MOG immunization, and this expansion of the Treg population may contribute to the attenuation of EAE.

To clarify whether MK affected the Treg cell population expansion directly, we assessed the antigen-specific expansion of the Treg cells *ex vivo*. Splenic $CD4^+$ T cells isolated from WT mice at peak MOG-EAE were stimulated with MOG peptide for 3 days *in vitro*. MK administration significantly decreased the Treg cell percentage and the *Foxp3* expression level in a dose-dependent manner (Fig. 3 *c* and *d*). STAT5 was recently demonstrated to be essential for Foxp3 expression and critical for both $CD4^+CD25^+$ Treg cell development and maintenance (22, 23). As shown in Fig. 3*e*, MK diminished the phosphorylation of STAT5 in a dose-dependent manner. Because STAT3 is reported to be critical for IL-6-dependent attenuation of Foxp3 expression (23), we assessed whether MK affects STAT3 phosphorylation. However, MK did not affect STAT3 phosphorylation in $CD4^+CD25^+$ cells (data not shown). Recent studies revealed that tyrosine phosphatase SHP-2 is a critical suppressor of STAT5 (24). MK enhanced the expression of SHP-2, and the inhibition of SHP-2 restored STAT5 phosphorylation and subsequent Foxp3 expression suppressed by MK (Fig. 3 *f* and *g*). These data indicate that MK deficiency contributes to the expansion of the Treg cell population through the dephosphorylation of STAT5 by SHP-2.

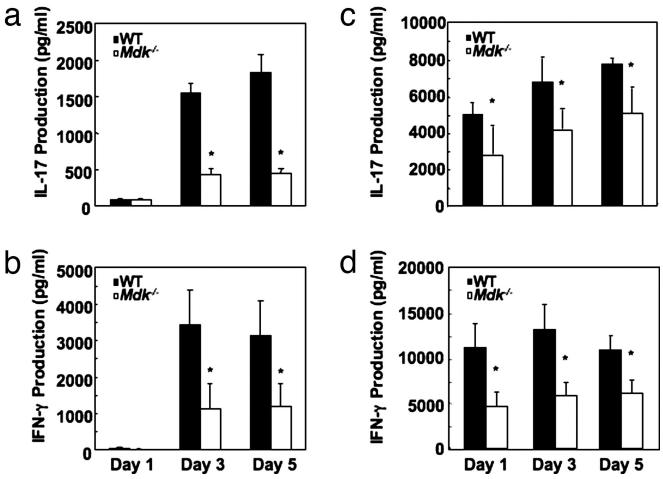

Fig. 4. MK deficiency attenuates the activation of autoreactive T_H1 and T_H17 cells. (*a–d*) The production of each of the examined cytokines by $MOG_{35–55}$-specific $CD4^+$ T cells from EAE mice was assessed with ELISAs. The production of the T_H17 cytokine IL-17 and the T_H1 cytokine IFN-γ in the spleen (*a* and *b*) and the CNS (*c* and *d*) was significantly lower in $Mdk^{-/-}$ mice (open bars) than in WT mice (filled bars). Data represent the means ± SD ($n = 6$). *, $P < 0.05$ versus WT.

Because EAE is a T_H1 and/or T_H17 cell-mediated autoimmune disease, we next examined whether the resistance to EAE in the $Mdk^{-/-}$ mice was associated with the suppression of autoreactive T_H1 and T_H17 cell populations in the periphery and CNS. As shown in Fig. 4, significantly lower amounts of IFN-γ and IL-17 were produced in the MOG-specific $CD4^+$ T cells from the $Mdk^{-/-}$-EAE mice than in those cells from the WT-EAE mice ($P < 0.05$).

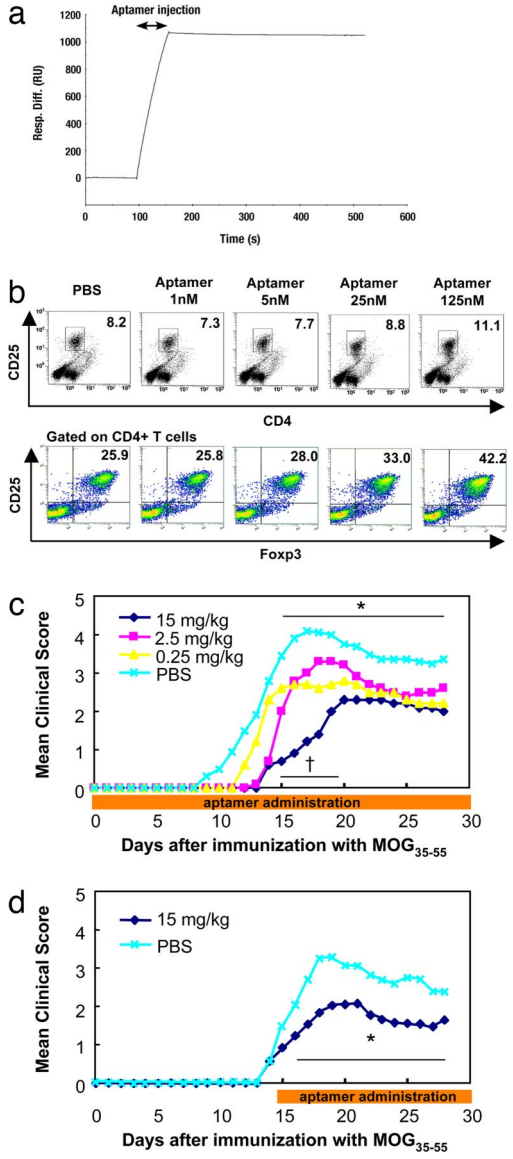

Fig. 5. Inhibition of MK signaling by neutralizing RNA aptamers suppresses EAE and is accompanied by an expansion of the Treg cell population. (*a*) A sensorgram of the RNA aptamers binding to MK. MK was immobilized on a CM4 sensor chip, and the RNA aptamers were injected during the indicated period. The K_d was estimated to be 0.9 nM by using global fitting curves (1:1 Langmuir binding) with four different RNA concentrations (0.05, 0.1, 0.2, and 0.4 μM). (*b*) Flow-cytometric analysis of the expansion of the Treg cell population using the anti-MK RNA aptamers *in vitro*. (*c*) Clinical scores for WT EAE mice administered 0 ($n = 9$), 0.25 ($n = 5$), 2.5 ($n = 5$), or 15 mg/kg ($n = 5$) anti-MK RNA aptamers from the day of immunization. Data represent the means ± SD. *, $P < 0.05$ for 0.25, 2.5, or 15 mg/kg anti-MK aptamers versus PBS. †, $P < 0.05$ for 15 mg/kg versus 0.25 or 2.5 mg/kg anti-MK aptamers. (*d*) Clinical scores for WT EAE mice administered PBS ($n = 10$) or 15 mg/kg ($n = 10$) anti-MK RNA aptamers after EAE onset (14 days after immunization). Data represent the means ± SD. *, $P < 0.05$ for 15 mg/kg anti-MK aptamers versus PBS.

In contrast, the MOG-specific $CD4^+$ T cells from the $Mdk^{-/-}$-EAE mice did not produce a detectable amount of the T_H2 cytokine IL-4, as was not observed for WT-EAE mice (data not shown). These data indicate that the autoreactive T_H1 and T_H17 cell populations were suppressed in the $Mdk^{-/-}$-EAE mice, but not in the WT-EAE mice. Therefore, we believe that MK serves as a critical suppressor of Treg cell expansion, and MK deficiency ameliorates EAE by expanding the population of Treg cells, which correspondingly suppresses the autoreactive T_H1 and T_H17 cell populations.

RNA Aptamer-Based Inhibition of MK Effectively Suppresses EAE. We next attempted to develop a therapeutic approach to treat EAE/MS using RNA aptamers that blocked MK function. Aptamer-based therapies have recently attracted attention as alternatives to antibody therapies (25–27). The anti-MK RNA aptamer used in this study was a 49-mer that was stabilized with ribose-2′ modifications, as well as cholesterol and inverted dT tags at its 5′ and 3′ ends, respectively (S.M., M.F., and Y.N., unpublished data). The apparent dissociation constant (K_d) estimated from the surface plasmon resonance (SPR) profile was 0.9 nM (Fig. 5*a*). RNA aptamers have been reported to overcome several disadvantages associated with therapeutic antibodies, such as neutralization, batch-to-batch variation, production limitations, and total cost. As expected, the administration of anti-MK RNA aptamers induced expansion of the Treg cell population and reduced the mean EAE clinical score in a dose-dependent manner (Fig. 5 *b* and *c*). Moreover, the aptamers administered after EAE onset also diminished the EAE clinical score (Fig. 5*d*). The results suggest that aptamer-based inhibition of MK is an alternative to therapeutic antibodies for the treatment of autoimmune diseases, such as MS.

Discussion

The present study demonstrates that MK is a critical suppressor of Treg cell expansion. We have shown that MK deficiency reduces the severity of EAE through an expansion of the Treg population in peripheral lymph nodes, followed by decreases in the numbers of autoreactive T_H1 and T_H17 cells. MK signaling is mediated by MK receptors, including protein-tyrosine phosphatase ζ, low-density lipoprotein receptor-related protein, anaplastic leukemia kinase, and syndecan-3 (1). Downstream signaling of MK activates the PI3K, PKC, and MAPK MEK1/2 pathways. These signaling pathways are thought to be associated with various functions that involve MK, including inflammatory cell migration and activation. MK is up-regulated in inflammatory cells, including activated macrophages, neutrophils, and T cells (1–4, 28). Thus, recent studies have proposed that the antiinflammatory condition resulting from MK deficiency was due to the loss of cytokine/chemokine-mediated migration signals directed at inflammatory cells (2–4). In the present study, however, we have revealed that loss of MK signaling attenuates EAE mainly via expansion of the Treg cell population because Treg cell depletion using anti-CD25 monoclonal antibodies completely cancelled the suppression of EAE in $Mdk^{-/-}$ mice. Moreover, we demonstrated that MK reduces the expansion of the Treg cell population *ex vivo*. A previous report showed that MK expression is up-regulated in the spinal cord during the induction and progression phases of EAE and then returns to a normal level during the recovery phase (5). However, an increased number of Treg cells is reportedly associated with recovery from EAE (29, 30). Taken together, these results suggest that MK participates in the induction and progression of EAE through the suppression of the Treg cell population.

Treg cells are believed to play a pivotal role in immunological homeostasis, and the suppression and/or dysregulation of Treg cells can induce autoimmune and inflammatory disorders, such as MS (11–13, 15, 18, 19). Recent studies showed that STAT5 is essential for IL-2-dependent Foxp3 expression and critical for both Treg cell development and maintenance (22, 23). STAT3 also is documented to be critical for IL-6-dependent attenuation of Foxp3 expression (23). Thus, STAT5 and STAT3 are considered to have opposing roles in regulating Foxp3; however, the factors that regulate Treg cells are still largely unknown. In this study, we demonstrated that MK decreases Treg cell population by the suppression of IL-2-dependent STAT5 phosphorylation and Foxp3 expression through the up-regulation of SHP-2 (SI Fig. 8), whereas MK did not alter STAT3 phosphorylation. Although MK signaling participates in the PI3K, PKC, and MAPK MEK1/2 pathways, we were not able to identify which pathway enhances SHP-2 (data not shown). Further

investigation is needed to elucidate the detailed molecular mechanism of this process.

Recent studies have revealed that estrogen (31–34), vasoactive intestinal peptide (VIP) (35, 36), and CD28 superagonist (37–39) induce the expansion of the Treg cell population. Although administration of estrogen, VIP, or CD28 superagonist could potentially relieve autoimmune diseases by increasing Treg cell numbers, these molecules are associated with a number of adverse effects that must be considered (estrogen: feminization, thrombosis, and oncogenesis; VIP: watery diarrhea, hypokalemia, and achlorhydria; CD28 superagonist: cytokine storm syndrome leading to fatality). MK deficiency, in contrast, does not result in any significant adverse abnormalities or symptoms (1).

In this study, we inhibited MK activity with anti-MK RNA aptamers. Aptamers are single-stranded oligonucleotides synthesized *in vitro* using an RNA selection-amplification protocol referred to as systematic evolution of ligands by exponential amplification (SELEX) (25–27). Aptamers are isolated from randomized RNA libraries as high-affinity oligonucleotides that recognize a wide range of target molecules with affinities and specificities that are comparable to those of antibodies. Although antibody therapy is a potent therapeutic strategy, the characteristics of RNA aptamers circumvent several disadvantages associated with therapeutic antibodies. First, unlike therapeutic antibodies, aptamers do not trigger an immune response that could neutralize the introduced molecules. Second, the process by which aptamers are chemically synthesized allows large amounts of aptamers to be produced without batch-to-batch variations. Third, aptamers are amenable to various chemical modifications, including organ-targeting signals. Fourth, the chemical synthesis process can reduce total production cost of aptamers, compared with that of therapeutic antibodies. Therefore, aptamer-based therapy is a potent therapeutic strategy that may replace many antibody therapies in the future. Recently, the U.S. Food and Drug Aministration approved antivascular endothelial growth factor aptamer as the treatment for age-related macular degeneration (40). Our study also provides strong evidence for the clinical efficacy of RNA aptamers.

Methods

Reagents. MOG peptide 35–55 ($MOG_{35–55}$; MEVGWYRSPFSRVVHLYRNGK) was synthesized and purified by Operon Biotechnologies. Incomplete Freund's adjuvant was obtained from Sigma–Aldrich. Heat-killed *Mycobacterium tuberculosis* H37Ra was obtained from Difco, and pertussis toxin was obtained from List Biological Laboratories. Anti-MK RNA aptamers were developed by Ribomic essentially as described previously (41). In brief, RNA aptamers were raised against MK by sing SELEX. The functionally optimized 49-mer RNA was modified with fluorine and *O*-methyl at the 2′ position of each ribose and with a cholesterol moiety and inverted dT tags at the 5′ and 3′ ends, respectively (S.M., M.F., and Y.N., unpublished data). The RNA administered to the animals was chemically synthesized (Gene Design). The antibodies used are as follows: PE-Cy5-anti-mouse CD4 (GK1.5; BD Pharmingen), PE-anti mouse CD8 (53–6.7; BD Pharmingen), PE-anti-mouse CD11b (M1/70; BD Pharmingen), PE-anti-mouse CD25 (PC61 or 7D4; BD Pharmingen), FITC-anti-mouse CD40 (HM40–3; BD Pharmingen), PE-anti-mouse B7–1 (CD80, 16–10A1; BD Pharmingen), FITC-anti-mouse B7–2 (CD86, GL-1; BD Pharmingen), anti-mouse-MHC Class II I-A/I-E (2G9; BD Pharmingen), FITC-anti-mouse Foxp3 (FJK-16s; eBiosciences), PE-anti-phospho-STAT3 (pY705), and PE-anti-phospho-STAT5 (pY694) (BD Pharmingen) anti-mouse SHP-2 antibody (Cell Signaling).

SPR Analysis. The SPR assays were performed essentially as described previously (42) using a Biacore 2000 instrument, except that MK was immobilized on a CM4 sensor chip via amino coupling (≈1,000 RUs). Curves closely fit to the sensorgrams were calculated as global fitting curves (1:1 Langmuir binding) generated by using the BIAevaluation 3.0 software (Biacore to estimate the K_d value).

Animals. The protocols for animal experiments were approved by the Animal Experiment Committee of Nagoya University. C57BL/6J mice deficient for the MK gene (*Mdk*) were generated as described previously (43). After backcrossing $Mdk^{+/-}$ mice to C57BL/6J mice for >10 generations, $Mdk^{+/-}$ mice were mated with each other to generate $Mdk^{+/+}$ and $Mdk^{-/-}$ mice, which were used in the present study. All experiments were performed with $Mdk^{+/+}$ and $Mdk^{-/-}$ littermates.

Active Induction of MOG-EAE. MOG-EAE mice were produced and assessed as described previously (20).

MK Administration with an s.c.-Implanted Microosmotic Pump. We administrated MK to mice with s.c.-implanted microosmotic pumps as described previously (3). Briefly, MK dissolved in PBS at a concentration of 1 mg/ml was loaded into a microosmotic pump (model 1002; Durect), which released 0.25 μl of the solution per hour of MK for 14 days. A pump containing PBS (vehicle control) or MK (treated group) was implanted s.c. under anesthesia on the day of immunization. For some experiments, mice underwent sham operations (operated control) and were used instead of the vehicle control mice.

***In Vivo* Depletion of Treg Cells.** To deplete the Treg cell population *in vivo*, mice were i.p. injected with 250 μg of purified anti-CD25 monoclonal antibodies (PC61) as described previously (44, 45). Control animals received PBS or rat IgG (Jackson ImmunoResearch). Four days later, peripheral blood mononuclear cells or splenocytes were analyzed for the lack of $CD4^+CD25^+$ T cells after labeling the cells with anti-CD4 and anti-CD25 monoclonal antibodies (7D4), which bind to CD25 noncompetitively with PC61.

Administration of anti-MK Neutralizing anti-MK RNA Aptamers. Mice were i.p. injected with the indicated doses of anti-MK RNA aptamers every other day from the day of MOG immunization or EAE onset (≈14 days after immunization).

Histological Analysis. Mice with peak EAE were anesthetized and perfused transcardially with 4% paraformaldehyde (PFA) in 0.1 M PBS. Lumbosacral spinal cords were immediately removed, postfixed in 4% PFA, and embedded in paraffin. Five-micrometer-thick sections were stained with H&E by using standard procedures. Stained sections were observed under a microscope.

***In Vitro* Priming of MOG-Specific $CD4^+$ T Cells.** Mononuclear cells were collected from the spleen and CNS as described previously (46). $CD4^+$ or $CD4^+CD25^+$ T cells were purified with magnetic cell sorting according to the manufacturer's protocols (Miltenyi Biotec). The purities of the $CD4^+$ and $CD4^+CD25^+$ T cell samples were >97% as determined by CD4- or CD25-specific immunostaining. Purified $CD4^+$ T cells (2×10^5 cells per well) isolated from the spleens or CNS of peak EAE mice were cultured with mitomycin C-treated feeder cells (5×10^6 cells per well) in the presence of 20 ng/ml $MOG_{35–55}$ for 1, 3, and 5 days. The concentrations of IL-17, IFN-γ, and IL-4 in the culture supernatant were assessed by using the corresponding cytokine-specific ELISA kits (IL-17, R & D Systems; IFN-γ and IL-4, BD Pharmingen) as described previously (20). To examine the effect of MK on the Treg cell population, cells stimulated with 20 ng/ml $MOG_{35–55}$ for 3 days in the presence of 0, 20, or 100 ng/ml MK were analyzed by flow cytometry. To evaluate T cell proliferation, purified $CD4^+CD25^+$ T cells isolated from the spleens of peak EAE mice were cultured at different ratios (0.1:1, 0.3:1, and 1:1) with $CD4^+CD25^-$ T cells in the presence of mitomycin C-treated feeder cells (5×10^6 cells per well) and 20 ng/ml $MOG_{35–55}$ for 3 days. T cell proliferation was assessed by using a mouse IL-2 ELISA kit (BD Pharmingen) as described previously (20).

Flow Cytometry. Cells were isolated from spleens, mesenteric lymph nodes, and popliteal lymph nodes. RBCs were removed from the samples with lysis buffer (Dako). To evaluate the phosphorylation of STATs, cells were pretreated with each inhibitor (MEK1/2 inhibitor PD98059, PI3K inhibitor wortmannin, PKC inhibitor staurosporin, or SHP-2 inhibitor; Calbiochem) for 3 h. Cells were subsequently incubated with 100 ng/ml MK for 15 min, followed by a 5-min treatment of 20 ng/ml IL-2. Then cells were collected in Cytefix/Cyteperm (BD Pharmingen) containing phosphatase inhibitor mixture (Sigma–Aldrich). To prevent nonspecific binding, cells were incubated with anti-mouse FcγIII/II receptor monoclonal antibodies (2.4G2; BD Pharmingen) at 4°C for 30 min. Then cells were labeled with the specific antibodies for 30 min at 4°C, followed by analysis with a flow cytometer (Cytomics FC500; Beckman Coulter) as described (21).

Western Blotting. Cells were lysed in TNES buffer [50 mM Tris·HCl (pH 7.5), 150 mM NaCl, 1% Nonidet P-40, 2 mM EDTA, and 0.1% SDS] with a protease inhibitor mixture (Roche Diagnostics) and a phosphatase inhibitor mixture (Sigma–Aldrich); 10 μg of protein from the total lysate was examined for Western blot analysis as described (47).

Analysis of Microglia and Macrophages. Mouse primary microglia were isolated from primary mixed glial cell cultures, which were obtained from newborn mice using the shaking-off method described previously in ref. 48. Peritoneal macro-

phages were prepared from mice that had received an i.p. injection of thioglycolate 72 h before collection. Macrophages were cultured in the same medium as the microglia. Microglia and peritoneal macrophages (1×10^6 cells per ml) were cultured in 24-well plates with or without 1 μg/ml LPS plus 1 ng/ml IFN-γ for 24 h in the presence of 250 ng/ml MK. Total RNA was extracted from the cells by using an RNeasy Mini-Kit according to the manufacturer's protocol (Qiagen). First-strand cDNA was generated from 5 μg of total RNA by using SuperScript II (Invitrogen). mRNA expression of antigen-presenting molecules (MHC class II, B7–1, B7–2, ICAM-1, and VCAM-1), cytokines (TNF-α, IL-1β, IL-6, IL-12p40, and IL-12p35), chemokines (IP-10, RANTES, MIP-1α, and MCP-1), and iNOS was assessed by using semiquantitative PCRs as described (49). All experiments were carried out in six independent trials.

Real-Time RT-PCR Analysis of Foxp3 Expression. Real-time RT-PCR analysis was carried out by using an ABI Prism 7000 sequence detection system (Applied Biosystems) as described previously (50). The relative expression levels of *Foxp3* were determined by normalization to the *GAPDH* expression level. The primer sequences used were as follows: Foxp3 forward, 5′-TTCATGCATCAGCTCTCCAC-3′; Foxp3 reverse, 5′-CTGGACACCCATTCCAGACT-3′; GAPDH forward, 5′-ACTCACGGCAAATTCAACG-3′; and GAPDH reverse, 5′-CCCTGTTGCTGTAGC-CGTA-3′. All experiments were carried out in six independent trials.

Statistical Analysis. The data were analyzed with Statview software version 5 (SAS Institute) using unpaired Student's *t* tests or one-way ANOVA with a Tukey–Kramer post hoc test.

ACKNOWLEDGMENTS. This work was supported in part by a Neuroimmunological Disease Research Committee grant from the Ministry of Health, Labour and Welfare of Japan (to A.S.); a grant-in-aid for JSPS fellows (to J.W.); a grant-in-aid for young scientists (to H.T.); a grant-in-aid for a 21st Century Center of Excellence program (to A.S.) from the Ministry of Education, Culture, Sports, Science and Technology of Japan; a Collaborative Development of Innovative Seeds grant (to A.S.); a Core Research for Evolution Science and Technology grant from the Japan Science and Technology Agency (to Y.N.); and a grant-in-aid for the RNA Information Network from the Ministry of Education, Culture, Sports, Science and Technology of Japan (to Y.N.).

1. Muramatsu T (2002) Midkine and pleiotrophin: Two related proteins involved in development, survival, inflammation and tumorigenesis. *J Biochem (Tokyo)* 132:359–371.
2. Sato W, *et al*. (2001) Midkine is involved in neutrophil infiltration into the tubulointerstitium in ischemic renal injury. *J Immunol* 167:3463–3469.
3. Horiba M, *et al*. (2000) Neointima formation in a restenosis model is suppressed in midkine-deficient mice. *J Clin Invest* 105:489–495.
4. Maruyama K, Muramatsu H, Ishiguro N, Muramatsu T (2004) Midkine, a heparin-binding growth factor, is fundamentally involved in the pathogenesis of rheumatoid arthritis. *Arthritis Rheum* 50:1420–1429.
5. Liu X, Mashour GA, Webster HF, Kurtz A (1998) Basic FGF, FGF receptor 1 are expressed in microglia during experimental autoimmune encephalomyelitis: Temporally distinct expression of midkine and pleiotrophin. *Glia* 24:390–397.
6. Hemmer B, Archelos JJ, Hartung HP (2002) New concepts in the immunopathogenesis of multiple sclerosis. *Nat Rev Neurosci* 3:291–301.
7. Mangan PR, *et al*. (2006) Transforming growth factor-beta induces development of the T (H)17 lineage. *Nature* 441:231–234.
8. Bettelli E, *et al*. (2006) Reciprocal developmental pathways for the generation of pathogenic effector TH17 and regulatory T cells. *Nature* 441:235–238.
9. Weaver CT, *et al*. (2006) Th17: An effector CD4 T cell lineage with regulatory T cell ties. *Immunity* 24:677–688.
10. Ivanov II, *et al*. (2006) The orphan nuclear receptor RORgammat directs the differentiation program of proinflammatory IL-17+ T helper cells. *Cell* 126:1121–1133.
11. Baecher-Allan C, Hafler DA (2004) Suppressor T cells in human diseases. *J Exp Med* 200:273–276.
12. Matarese G, *et al*. (2005) Leptin increase in multiple sclerosis associates with reduced number of CD4(+)CD25+ regulatory T cells. *Proc Natl Acad Sci USA* 102:5150–5155.
13. Viglietta V, Baecher-Allan C, Weiner HL, Hafler DA (2004) Loss of functional suppression by CD4+CD25+ regulatory T cells in patients with multiple sclerosis. *J Exp Med* 199:971–979.
14. Kohm AP, Carpentier PA, Anger HA, Miller SD (2002) Cutting edge: CD4+CD25+ regulatory T cells suppress antigen-specific autoreactive immune responses and central nervous system inflammation during active experimental autoimmune encephalomyelitis. *J Immunol* 169:4712–4716.
15. Sakaguchi S (2004) Naturally arising CD4+ regulatory T cells for immunologic self-tolerance and negative control of immune responses. *Annu Rev Immunol* 22:531–562.
16. Sakaguchi S (2005) Naturally arising Foxp3-expressing CD25+CD4+ regulatory T cells in immunological tolerance to self and non-self. *Nat Immunol* 6:345–352.
17. Liu H, Leung BP (2006) CD4+CD25+ regulatory T cells in health and disease. *Clin Exp Pharmacol Physiol* 33:519–524.
18. Mills KH (2004) Regulatory T cells: Friend or foe in immunity to infection? *Nat Rev Immunol* 4:841–855.
19. von Herrath MG, Harrison LC (2003) Antigen-induced regulatory T cells in autoimmunity. *Nat Rev Immunol* 3:223–232.
20. Kato H, *et al*. (2004) Pituitary adenylate cyclase-activating polypeptide (PACAP) ameliorates experimental autoimmune encephalomyelitis by suppressing the functions of antigen presenting cells. *Mult Scler* 10:651–659.
21. Takeuchi H, *et al*. (2006) Interferon-gamma induces microglial-activation-induced cell death: A hypothetical mechanism of relapse and remission in multiple sclerosis. *Neurobiol Dis* 22:33–39.
22. Burchill MA, *et al*. (2007) IL-2 receptor beta-dependent STAT5 activation is required for the development of Foxp3+ regulatory T cells. *J Immunol* 178:280–290.
23. Yao Z, *et al*. (2007) Nonredundant roles for Stat5a/b in directly regulating Foxp3. *Blood* 109:4368–4375.
24. Yu CL, Jin YJ, Burakoff SJ (2000) Cytosolic tyrosine dephosphorylation of STAT5. Potential role of SHP-2 in STAT5 regulation. *J Biol Chem* 275:599–604.
25. Wilson DS, Szostak JW (1999) *In vitro* selection of functional nucleic acids. *Annu Rev Biochem* 68:611–647.
26. Brody EN, Gold L (2000) Aptamers as therapeutic and diagnostic agents. *J Biotechnol* 74:5–13.
27. Mori T, Oguro A, Ohtsu T, Nakamura Y (2004) RNA aptamers selected against the receptor activator of NF-kappaB acquire general affinity to proteins of the tumor necrosis factor receptor family. *Nucleic Acids Res* 32:6120–6128.
28. Callebaut C, *et al*. (2001) Inhibition of HIV infection by the cytokine midkine. *Virology* 281:248–264.
29. McGeachy MJ, Stephens LA, Anderton SM (2005) Natural recovery and protection from autoimmune encephalomyelitis: Contribution of CD4+CD25+ regulatory cells within the central nervous system. *J Immunol* 175:3025–3032.
30. Zhang X, *et al*. (2006) Recovery from experimental allergic encephalomyelitis is TGF-beta dependent and associated with increases in CD4+LAP+ and CD4+CD25+ T cells. *Int Immunol* 18:495–503.
31. Polanczyk MJ, *et al*. (2004) Cutting edge: Estrogen drives expansion of the CD4+CD25+ regulatory T cell compartment. *J Immunol* 173:2227–2230.
32. Reddy J, *et al*. (2004) Myelin proteolipid protein-specific CD4+CD25+ regulatory cells mediate genetic resistance to experimental autoimmune encephalomyelitis. *Proc Natl Acad Sci USA* 101:15434–15439.
33. Polanczyk MJ, *et al*. (2005) Enhanced FoxP3 expression and Treg cell function in pregnant and estrogen-treated mice. *J Neuroimmunol* 170:85–92.
34. Reddy J, *et al*. (2005) Cutting edge: CD4+CD25+ regulatory T cells contribute to gender differences in susceptibility to experimental autoimmune encephalomyelitis. *J Immunol* 175:5591–5595.
35. Fernandez-Martin A, *et al*. (2006) Vasoactive intestinal peptide induces regulatory T cells during experimental autoimmune encephalomyelitis. *Eur J Immunol* 36:318–326.
36. Gonzalez-Rey E, *et al*. (2006) Therapeutic effect of vasoactive intestinal peptide on experimental autoimmune encephalomyelitis: Down-regulation of inflammatory and autoimmune responses. *Am J Pathol* 168:1179–1188.
37. Beyersdorf N, *et al*. (2005) Selective targeting of regulatory T cells with CD28 superagonists allows effective therapy of experimental autoimmune encephalomyelitis. *J Exp Med* 202:445–455.
38. Beyersdorf N, Hanke T, Kerkau T, Hunig T (2006) CD28 superagonists put a break on autoimmunity by preferentially activating CD4+CD25+ regulatory T cells. *Autoimmun Rev* 5:40–45.
39. Suntharalingam G, *et al*. (2006) Cytokine storm in a phase 1 trial of the anti-CD28 monoclonal antibody TGN1412. *N Engl J Med* 355:1018–1028.
40. Que-Gewirth NS, Sullenger BA (2007) Gene therapy progress and prospects: RNA aptamers. *Gene Ther* 14:283–291.
41. Oguro A, *et al*. (2003) RNA aptamers to initiation factor 4A helicase hinder cap-dependent translation by blocking ATP hydrolysis. *RNA* 9:394–407.
42. Miyakawa S, *et al*. (2006) RNA aptamers to mammalian initiation factor 4G inhibit cap-dependent translation by blocking the formation of initiation factor complexes. *RNA* 12:1825–1834.
43. Nakamura E, *et al*. (1998) Disruption of the midkine gene (Mdk) resulted in altered expression of a calcium binding protein in the hippocampus of infant mice and their abnormal behaviour. *Genes Cells* 3:811–822.
44. Nishikawa H, *et al*. (2003) CD4+ CD25+ T cells responding to serologically defined autoantigens suppress antitumor immune responses. *Proc Natl Acad Sci USA* 100:10902–10906.
45. Nishikawa H, *et al*. (2005) Accelerated chemically induced tumor development mediated by CD4+CD25+ regulatory T cells in wild-type hosts. *Proc Natl Acad Sci USA* 102:9253–9257.
46. Sonobe Y, *et al*. (2007) Chronological changes of CD4(+) and CD8(+) T cell subsets in the experimental autoimmune encephalomyelitis, a mouse model of multiple sclerosis. *Tohoku J Exp Med* 213:329–339.
47. Takeuchi H, *et al*. (2002) Mitochondrial localization of mutant superoxide dismutase 1 triggers caspase-dependent cell death in a cellular model of familial amyotrophic lateral sclerosis. *J Biol Chem* 277:50966–50972.
48. Suzumura A, Mezitis SG, Gonatas NK, Silberberg DH (1987) MHC antigen expression on bulk isolated macrophage–microglia from newborn mouse brain: Induction of Ia antigen expression by gamma-interferon. *J Neuroimmunol* 15:263–278.
49. Kawanokuchi J, *et al*. (2004) Effects of interferon-beta on microglial functions as inflammatory and antigen presenting cells in the central nervous system. *Neuropharmacology* 46:734–742.
50. Sonobe Y, *et al*. (2005) Production of IL-27 and other IL-12 family cytokines by microglia and their subpopulations. *Brain Res* 1040:202–207.